IEEE Photonics Journal
An IEEE Photonics Society Publication

Four Wave Mixing-Based Time Lens for Orthogonal Polarized Input Signals

Volume 9, Number 2, April 2017

Avi Klein
Shir Shahal
Gilad Masri
Hamootal Duadi
Moti Fridman

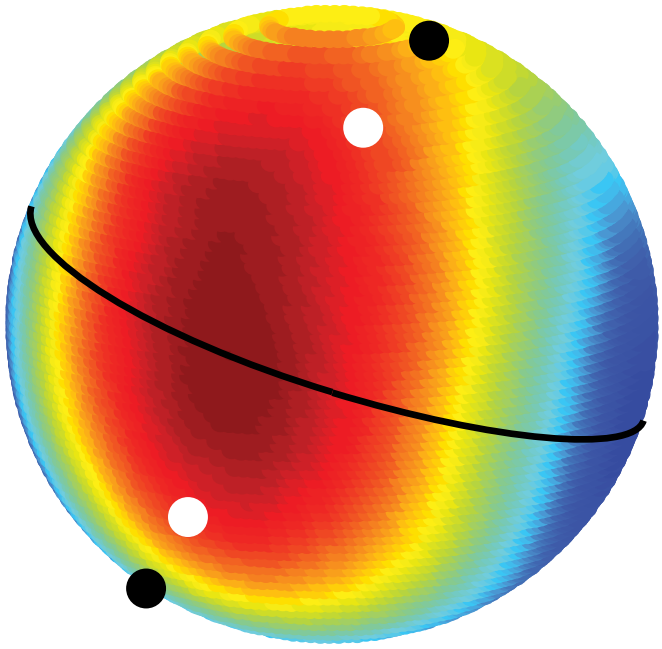

DOI: 10.1109/JPHOT.2017.2690899
1943-0655 © 2017 IEEE

IEEE photonics SOCIETY

IEEE

Four Wave Mixing-Based Time Lens for Orthogonal Polarized Input Signals

Avi Klein, Shir Shahal, Gilad Masri, Hamootal Duadi, and Moti Fridman

Faculty of Engineering, Institute of Nanotechnology and Advanced Materials, Bar Ilan University, Ramat Gan 5290002, Israel

DOI:10.1109/JPHOT.2017.2690899

Manuscript received February 19, 2017; revised March 31, 2017; accepted April 1, 2017. Date of publication April 7, 2017; date of current version April 19, 2017. This work was supported in part by the KAMIN program under the office of the chief scientist in Israel. Corresponding author: M. Fridman (e-mail: moti43@gmail.com).

Abstract: We present highly efficient time-lenses for orthogonal polarized signal waves with a specific state of polarization. Our four-wave mixing based time-lenses exploit polarization mode dispersion to compensate for chromatic dispersion. The results reveal that the efficiency of the time-lens is increased fivefold for both states of polarization. We also compensate for any polarization-dependent losses in the system by tailoring the pump state of polarization. Our time-lenses can be implemented in current telecommunication systems together with polarization division multiplexing in order to reach higher bandwidth.

Index Terms: Fiber nonlinear optics, nonlinear optical devices, optical polarization.

1. Introduction

Telecommunication systems require increasing capacity to handle the exponential growth in bandwidth demand [1]. Several routes for increasing the bandwidth of current networks are being investigated [1]. Among them is polarization division multiplexing which doubles the capacity of communication systems by transmitting two orthogonal polarized signals on a single channel [2]. Another route for increasing the bandwidth is optical signal processing by time-lenses, which removes electronic bottlenecks from the network [3], [4]. However, current time-lenses, which are based on four-wave mixing, are polarization dependent and, therefore, can not be implemented together with polarization division multiplexing [5]–[7].

We present efficient time-lenses designed for inputs composed from two orthogonally polarized signals. Such time-lenses can be implemented together with polarization division multiplexing for improved telecommunication systems. The time-lens efficiency is increased fivefold by tailoring the pump wave state of polarization, so the polarization mode dispersion compensates for the chromatic dispersion [8], [9]. We also demonstrate how our time-lens compensates for polarization dependent losses along the telecommunication system. We note that our time-lens is designed for a specific input states of polarization and it is not a polarization insensitive time-lens.

Previous works on vectorial non-linearities suggested polarization independent FWM schemes based on two pump waves [7], [10], [11]. However, for time-lenses, where the relative phase between the idler waves is important, it is essential to base the time-lens on a single pump wave. We believe that such time-lenses can increase the bandwidth of current telecommunication systems and open

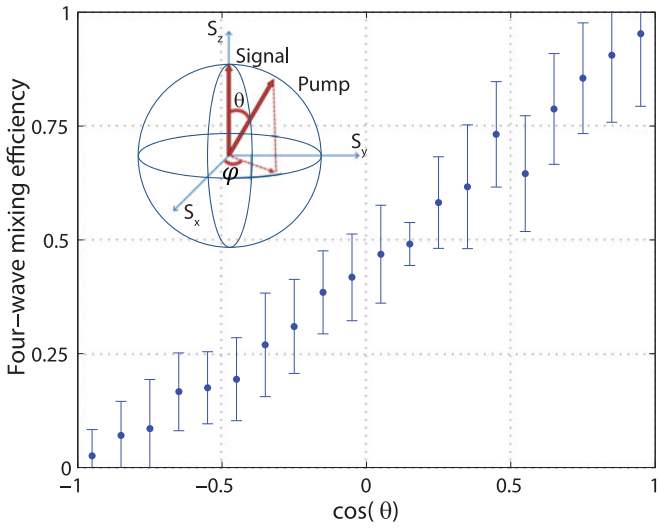

Fig. 1. Four-wave mixing efficiency as a function of the relative state of polarization between the signal and the pump waves. The relative state of polarization is denoted by the angle θ between the two Stokes vectors in the Poincare sphere representation, as presented in the inset. The results follow a linear curve according to (2).

an alternative route toward wide-bandwidth networks. With our time-lens, it is possible to investigate the output of lasers with two orthogonally polarized pulses such as fiber lasers with polarization instabilities or Raman coupled lasers [12], [13]. Also, our time-lens can lead to optical processing of orthogonal signals where the relative phase between the signals is important as is the case in quantum cryptography [14].

2. Theoretical Background

Temporal optics rises from the duality between diffraction and dispersion [15], [16]. Similar to a spatial lens which impart a quadratic phase shift in space, a time-lens imparts a quadratic phase shift in time on an input signal [16]–[19]. Time-lenses which are based on the four-wave mixing (FWM) process imparts a significantly larger phase shift [17]–[22]. Therefore, such time-lenses were implemented for compressing and stretching signals [4], for time-to-frequency mapping [23], [24] and for temporal cloaking [20]. In such time-lenses, an idler wave (E_i) is generated in a nonlinear process between a pump wave (E_p) and a signal wave (E_s) according to

$$E_i = \chi^{(3)} E_p^2 E_s^* \tag{1}$$

where $\chi^{(3)}$ is the third order nonlinear susceptibility of the material. The pump wave is chirped so its frequency changes linearly in time, which is equivalent to a quadratic phase shift. So, the resulting idler equals to the signal wave multiply by a quadratic phase shift.

The process of FWM is fast, robust, highly efficient, and impose strong phase changes. However, the FWM process is sensitive to the relative state of polarization of the signal wave compared to the pump wave. Thus, only the projected component of the signal state of polarization on the pump state of polarization interacts to produce the idler wave. Therefore, in a Poincare sphere representation, where orthogonal polarizations are denoted by anti-parallel Stokes vectors, the idler wave obeys

$$E_i = \chi^{(3)} E_p^2 E_s^* \frac{1+\cos(\theta)}{2} \tag{2}$$

where θ denotes the angle between the Stokes vectors of the signal and the pump waves, as presented in the inset of Fig. 1. We measured the FWM efficiency as a function of the relative state

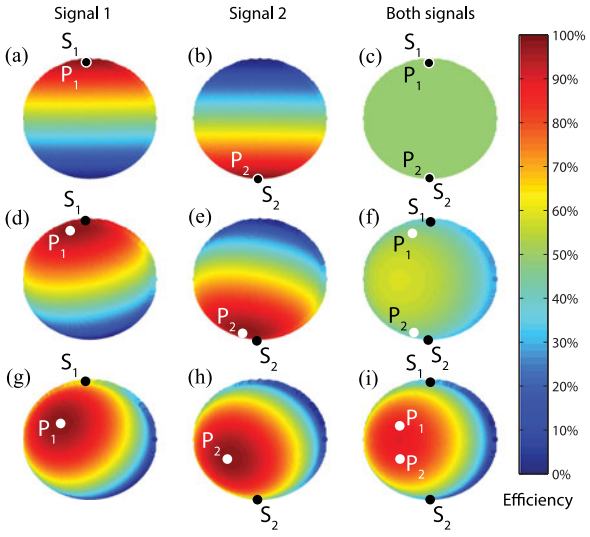

Fig. 2. Calculated FWM efficiency as a function of the pump state of polarization for different input signals. Each point is colored according to the FWM efficiency when the pump state of polarization is oriented toward that point in the Poincare sphere. Black dots denote the polarization orientation of the signal, and white dots denote the pump which gives the highest efficiency. The first and second columns present the efficiency when the input signal is S_1 and S_2, respectively, and the third column is the combined efficiency. In the first row, the polarization mode dispersion (PMD) is set to 0, and at the second and third rows, the PMD is set to 0.02 and 0.1 ps/$\sqrt{\text{km}}$, respectively.

of polarization between the signal and the pump waves and present the results in Fig. 1. As evident, the relative efficiency as a function of cos(θ) follows a linear curve as predicted by Eq. (2) [25], [26].

Thus, in time-lenses for signals composed from orthogonal polarized waves, the pump state of polarization should be between the two signals states of polarization, namely $\theta = \pi/2$ regardless of φ. Thus, obtaining 50% FWM efficiency for both polarized signal waves. These results are illustrated on the first row in Fig. 2. Every point on the Poincare sphere is colored according to the FWM efficiency for a pump oriented toward that state of polarization where red represent high efficiency and blue low efficiency. We assume, without loss of generality, that the polarization of one signal wave, S_1, is oriented toward the north pole, while the other signal wave, S_2, is oriented toward the south pole, which are the right circular and left circular states of polarization, respectively. Fig. 2(a) presents the FWM efficiency for every state of polarization of the pump, when the input signal wave is S_1 and its state of polarization is denoted by the black dot. The pump state of polarization which gives the highest efficiency is denoted by P_1 as the white dot. The results are consistent with Eq. (2) and Fig. 1 and state that the most efficient FWM process rise when the pump state of polarization is parallel to the signal state of polarization. Fig. 2(b) presents the same calculations for signal wave S_2, with similar results oriented toward the south pole. Fig. 2(c) presents the combined efficiency when both signal waves enter simultaneously into the FWM process. Here the combined efficiency is constant regardless of the pump state of polarization due to the linear curve in Fig. 1, so if the pump state of polarization is closer to one signal wave it is farther from the other one. However, to obtain equal efficiency of 50% from both signals, the pump state of polarization should be oriented toward the equator which represents linear states of polarization. The efficiency does not depends on the orientation of the linear polarization of the pump wave since it has the same efficiency along the equator.

When considering chromatic dispersion along the nonlinear fiber, the maximal FWM efficiency drops since the pump and the signal waves travel in different speeds and cannot overlap along the entire nonlinear fiber [8]. However, different states of polarization travel in different speeds as well, which is known as polarization mode dispersion (PMD) [27]. Thus, shifting the pump state of polarization so it will not be parallel to the signal state of polarization can compensate for the

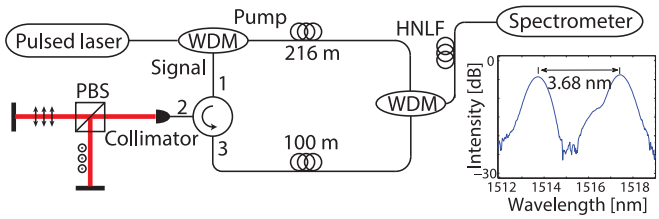

Fig. 3. Schematic layout of time-lens in a 2-f configuration for orthogonal polarized signal waves. CWDM: coarse wavelength division multiplexer. PBS: polarized beam splitter, HNLF: highly nonlinear fiber. (inset) Measured spectrum of the idler wave.

chromatic dispersion in the nonlinear fiber, so the pump and the signal waves will travel in the same speed which will increase the FWM efficiency [9]. These results are presented in the second and third rows of Fig. 2, where for the second row we included a PMD of 0.02 ps/$\sqrt{\text{km}}$ and for the third row a PMD of 0.1 ps/$\sqrt{\text{km}}$. The results of (d) and (e) reveal that the pump state of polarization with the highest efficiency is not parallel to the signal state of polarization anymore, but is shifted toward a preferable longitude. Thus, as presented in (f), now there is a preferable state of polarization for the pump when considering both signals together, namely a preferable φ. When increasing the PMD to 0.1 ps/$\sqrt{\text{km}}$, as presented in (g) and (h), the polarization of the pump with the highest efficiency shifts farther away from the signals states of polarization. Then, the combined efficiency for both signals at the preferable state of polarization is five times higher than the one at the lowest efficiency, as presented in (i).

With our method, it is possible to improve the time-lens efficiency as long as the signal wave state of polarization is not the principle states of polarization of the fiber. However, when the chromatic dispersion increases above the polarization mode dispersion, the efficiency improvement drops. We also note that higher order polarization mode dispersion can introduce chirping to the pump and the signal waves which can also reduce the efficiency of the time-lens.

3. Experimental Setup and Results

We build a time-lens in a 2-f configuration, for time-to-frequency conversion, designed for orthogonal polarized signal waves. Schematics of the experimental setup are presented in Fig. 3. A short pulse of 40 nm (FWHM) and a pulse width of 80 *fs* divides into a pump wave with a wavelength of 1531 $\pm$ 6.5 nm and a signal wave with a wavelength of 1551 $\pm$ 6.5 nm. The signal wave splits into two pulses with orthogonal states of polarization and a temporal separation of $\Delta\tau_s = 15$ ps by a polarizing beam splitter and mirrors on accurate translation stages separated by 2.2 mm. The Stokes vectors of the two signal pulses are: (0.45, 0.06, 0.89) and ($-$0.44, $-$0.36, $-$0.82). The pump and the signals are chirped by dispersion compensating fibers of 216 m and 100 m lengths (Thorlabs DCF-38) into a 40 ps and a 15 ps Gaussian pulses width, respectively. The pump pulse was timed between the two signal pulses for equal overlapping between each signal pulse and the pump wave. Then, the signal and the pump waves interact in a 1 *k*m highly nonlinear fiber (OFS standard HNLF) and the resulting idler wave is measured with an optical spectrum analyzer.

The measured idler spectrum, presented in the inset of Fig. 3, is composed from two peaks separated by $\Delta\lambda_i = 3.68$ nm generated from time-to-frequency conversion of the two temporal peaks in the signal wave $\Delta\tau_s = 15$ ps. These results agree with [28]

$$\Delta\tau_s = \left(\frac{\lambda_s}{\lambda_i}\right)^2 D\,L\,\Delta\lambda_i \tag{3}$$

where λ_s and λ_i are the wavelength of the signal and the idler waves respectively, D is the dispersion of the fiber and L is the length of the fiber. The intensity of the two idler peaks indicates the FWM efficiency where an efficient time-lens aims for higher and equal peaks.

We measured the FWM efficiency for each of the signal wave as a function of the pump wave state of polarization and present it in Fig. 4. Each point on the Poincare sphere is colored according to

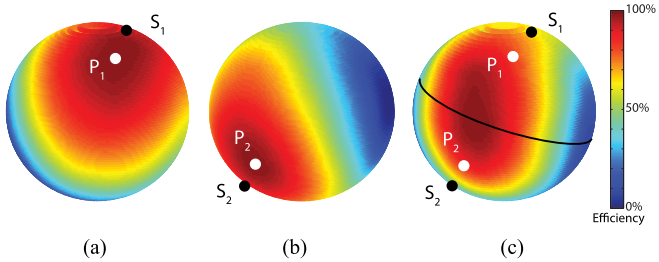

Fig. 4. Measured FWM efficiency as a function of the pump wave state of polarization. Each point in the Poincare spheres is colored according to the FWM efficiency when the pump polarization is oriented toward that point. (a) FWM efficiency when the input signal wave is S_1 denoted as the black dot, where the pump state of polarization with the highest efficiency is denoted as P_1 and the white dot. (b) Same measurements for S_2. (c) Combined efficiency when the input is both signal waves simultaneously. The black curve is composed from all the points with equal distances from S_1 and S_2 so that the efficiency along this curve is equal for both signal waves.

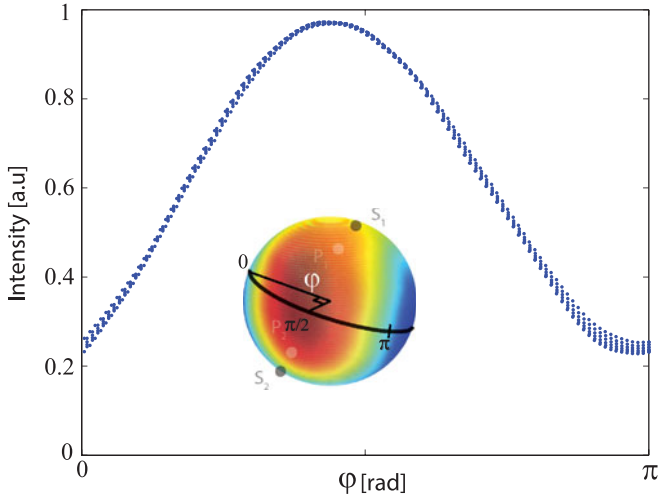

Fig. 5. Measured intensity of both idler waves along the black curve presented in the inset which is copy of Fig. 4(c).

the FWM efficiency when the pump state of polarization is oriented toward this point. Red indicates high efficiency while blue indicates low efficiency. Fig. 4(a) presents the FWM efficiency as a function of the pump state of polarization when the input signal wave is S_1 (black dot). The pump state of polarization with the highest efficiency is denoted as P_1 (white dot). Fig. 4(b) presents the same measurements for S_2 which is orthogonally polarized to S_1. Fig. 4(c) presents the combined efficiency for both signal waves together. To obtain equal FWM efficiency for both signal waves the pump state of polarization is oriented toward a curve between the two signals which is presented as the black curve. We plotted the FWM efficiency as a function of the orientation along the black curve and present it in Fig. 5. The results reveal that when the pump state of polarization is oriented at 0.45π the efficiency is five times higher than the efficiency when the polarization is oriented at π. Here, both idler waves have almost the same state of polarization; nevertheless, by resorting to polarization maintaining non-linear fiber with higher PMD, we hope to demonstrate idler waves with different states of polarization.

Finally, in many cases, the intensities of the two orthogonal signal waves are unequal due to polarization dependent losses, we show how our time-lens can compensate for such polarization dependent losses. We denote the intensities of the two signals as I_{s1} and I_{s2} and define the normalized difference between them as $\Delta I = (I_{s1} - I_{s2})/(I_{s1} + I_{s2})$. Measured results of the FWM

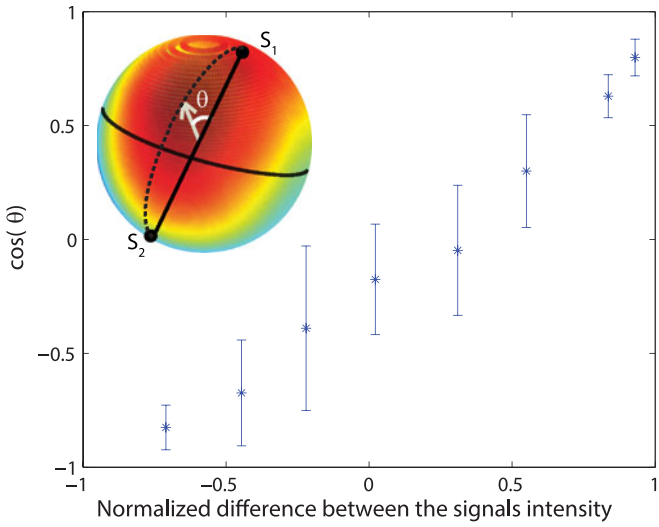

Fig. 6. Cosine of the angle θ as a function of the normalized intensity difference between the signal waves S_1 and S_2. (Inset) Measured results of the FWM efficiency as a function of the pump state of polarization for unequal signals intensities. Specifically, the intensity of S_1, is three times stronger than the intensity of s_2. This corresponds to a normalize intensity difference of $\Delta I = (I_{s1} - I_{s2})/(I_{s1} + I_{s2}) = 0.5$. The angle between the polarization with the highest efficiency and the north pole is denoted as θ, and in this pump state of polarization, both idler waves have the same intensity.

efficiency when $\Delta I = 0.5$ are presented in the inset of Fig. 6. As evident, the peak efficiency is shifted above the black curve, and in this pump state of polarization both idler waves have the same intensity although the unbalance in the signal waves intensities. We measured the angle θ as a function of ΔI and present it in Fig. 6. As evident, by shifting the pump state of polarization from the black curve it is possible to compensate for any polarization dependent losses with our time-lens and obtain idler waves with equal intensities.

4. Summary and Conclusion

To conclude, we developed an efficient time-lens for signals composed from orthogonally polarized waves. We showed how the efficiency can be increased fivefold by tailoring the pump wave state of polarization. The time-lens is based on compensating for the chromatic dispersion in the nonlinear fiber by exploiting polarization mode dispersion. We present calculated results to support our findings and showed that our time-lens can also compensate for any polarization dependent losses along the telecommunication system. Our time-lens can be implemented in current telecommunication systems together with polarization division multiplexing in order to reach higher bandwidth. Also, our time-lens can investigate pulsed lasers with two polarized pulses and can process signals composed from two orthogonal polarizations where the relative phase is important.

References

[1] E. Agrell *et al.*, "Roadmap of optical communications," *J. Opt.*, vol. 18, no. 6, 2016, Art. no. 063002. [Online]. Available: http://stacks.iop.org/2040-8986/18/i=6/a=063002
[2] A. H. Gnauck *et al.*, "25.6-Tb/s WDM transmission of polarization-multiplexed RZ-DQPSK signals," *J. Lightw. Technol.*, vol. 26, no. 1, pp. 79–84, Jan. 2008.
[3] M. A. Foster, R. Salem, D. F. Geraghty, A. C. Turner-Foster, M. Lipson, and A. L. Gaeta, "Silicon-chip-based ultrafast optical oscilloscope," *Nature*, vol. 456, no. 7218, pp. 81–84, 2008.
[4] R. Salem, M. A. Foster, A. C. Turner-Foster, D. F. Geraghty, M. Lipson, and A. L. Gaeta, "High-speed optical sampling using a silicon-chip temporal magnifier," *Opt. Exp.*, vol. 17, no. 6, pp. 4324–4329, 2009.
[5] G. Hunziker, R. Paiella, D. F. Geraghty, K. J. Vahala, and U. Koren, "Polarization-independent wavelength conversion at 2.5 Gb/s by dual-pump four-wave mixing in a strained semiconductor optical amplifier," *IEEE Photon. Technol. Lett.*, vol. 8, no. 12, pp. 1633–1635, Dec. 1996.

[6] B. Batagelj, M. Vidmar, and S. Tomazic, "Use of four-wave mixing in optical fibers for applications in transparent optical networks," in *Proc. 6th Int. Conf. Transparent Opt. Netw.*, 2004, vol. 1, pp. 215–220.
[7] Q. Lin and G. P. Agrawal, "Vector theory of four-wave mixing: Polarization effects in fiber-optic parametric amplifiers," *J. Opt. Soc. Amer. B*, vol. 21, no. 6, pp. 1216–1224, 2004.
[8] G. P. Agrawal, *Nonlinear Fiber Optics*. New York, NY, USA: Academic, 2007.
[9] M. Romagnoli, P. Franco, R. Corsini, A. Schiffini, and M. Midrio, "Time-domain fourier optics for polarization-mode dispersion compensation," *Opt. Lett.*, vol. 24, no. 17, pp. 1197–1199, Sep. 1999. [Online]. Available: http://ol.osa.org/abstract.cfm?URI=ol-24-17-1197
[10] T. Tanemura, K. Katoh, and K. Kikuchi, "Polarization-insensitive asymmetric four-wave mixing using circularly polarized pumps in a twisted fiber," *Opt. Exp.*, vol. 13, no. 19, pp. 7497–7505, Sep. 2005. [Online]. Available: http://www.opticsexpress.org/abstract.cfm?URI=oe-13-19-7497
[11] W. Yang, Y. Yu, M. Ye, G. Chen, C. Zhang, and X. Zhang, "Phase regeneration for polarization-division multiplexed signals based on vector dual-pump nondegenerate phase sensitive amplification," *Opt. Exp.*, vol. 23, no. 3, pp. 2010–2020, Feb. 2015. [Online]. Available: http://www.opticsexpress.org/abstract.cfm?URI=oe-23-3-2010
[12] V. Tsatourian *et al.*, "Polarisation dynamics of vector soliton molecules in mode locked fibre laser," *Sci. Rep.*, vol. 3, 2013, Art. no. 3154.
[13] H. Huang, D. Shen, and J. He, "Simultaneous pulse generation of orthogonally polarized dual-wavelength at 1091 and 1095 nm by coupled stimulated raman scattering," *Opt. Exp.*, vol. 20, no. 25, pp. 27838–27846, Dec. 2012. [Online]. Available: http://www.opticsexpress.org/abstract.cfm?URI=oe-20-25-27838
[14] L. Goldenberg and L. Vaidman, "Quantum cryptography based on orthogonal states," *Phys. Rev. Lett.*, vol. 75, pp. 1239–1243, Aug. 1995. [Online]. Available: http://link.aps.org/doi/10.1103/PhysRevLett.75.1239
[15] E. B. Treacy, "Optical pulse compression with diffraction gratings," *IEEE J. Quantum Electron.,* vol. QE-5, no. 9, pp. 454–458, Sep. 1969.
[16] S. Akhmanov, A. Chirkin, K. Drabovich, A. Kovrigin, R. Khokhlov, and A. Sukhorukov, "Nonstationary nonlinear optical effects and ultrashort light pulse formation," *IEEE J. Quantum Electron.,* vol. QE-4, no. 10, pp. 598–605, Oct. 1968.
[17] B. H. Kolner, "Space-time duality and the theory of temporal imaging," *IEEE J. Quantum Electron.,* vol. 30, no. 8, pp. 1951–1963, Aug. 1994.
[18] B. H. Kolner and M. Nazarathy, "Temporal imaging with a time-lens," *Opt. Lett.*, vol. 14, no. 12, pp. 630–632, 1989.
[19] N. Berger, B. Levit, S. Atkins, and B. Fischer, "Time-lens-based spectral analysis of optical pulses by electrooptic phase modulation," *Electron. Lett.*, vol. 36, no. 19, pp. 1644–1646, 2000.
[20] M. Fridman, A. Farsi, Y. Okawachi, and A. L. Gaeta, "Demonstration of temporal cloaking," *Nature*, vol. 481, no. 7379, pp. 62–65, 2012.
[21] M. Fridman, Y. Okawachi, S. Clemmen, M. Ménard, M. Lipson, and A. L. Gaeta, "Waveguide-based single-shot temporal cross-correlator," *J. Opt.*, vol. 17, no. 3, 2015, Art. no. 035501.
[22] C. V. Bennett and B. H. Kolner, "Principles of parametric temporal imaging. II. System performance," *IEEE J. Quantum Electron.,* vol. 36, no. 6, pp. 649–655, Jun. 2000.
[23] J. Azana, N. K. Berger, B. Levit, and B. Fischer, "Spectral fraunhofer regime: Time-to-frequency conversion by the action of a single time-lens on an optical pulse," *Appl. Opt.*, vol. 43, no. 2, pp. 483–490, 2004.
[24] C. Zhang, B. Li, and K. K.-Y. Wong, "Ultrafast spectroscopy based on temporal focusing and its applications," *IEEE J. Sel. Topics Quantum Electron.,* vol. 22, no. 3, May/Jun. 2016, Art. no. 6800312.
[25] T. Hasegawa, K. Inoue, and K. Oda, "Polarization independent frequency conversion by fiber four-wave mixing with a polarization diversity technique," *IEEE Photon. Technol. Lett.*, vol. 5, no. 8, pp. 947–949, Aug. 1993.
[26] S. Song, C. T. Allen, K. R. Demarest, and R. Hui, "A novel method for measuring polarization-mode dispersion using four-wave mixing," *J. Lightw. Technol.*, vol. 17, no. 12, pp. 2530–2533, Dec. 1999.
[27] Z. Wang, C. Xie, and X. Ren, "PMD and PDL impairments in polarization division multiplexing signals with direct detection," *Opt. Exp.*, vol. 17, no. 10, pp. 7993–8004, 2009.
[28] E. Ryckeboer, "Time-lens oscilloscope of optical signal packets by nonlinear optics," M.Sc. thesis, Univ. Gent, Belgium, 2009.